Pergamon

Geochimica et Cosmochimica Acta, Vol. 61, No. 22, pp. 4789–4797, 1997

0016-7037/97 $17.00 + .00

PII S0016-7037(97)00280-9

The correlation between the U^k_{37} index and sea surface temperatures in the warm boundary: The South China Sea

CARLES PELEJERO and JOAN O. GRIMALT*
Department of Environmental Chemistry (C.I.D.-C.S.I.C.), Jordi Girona, 18. 08034 Barcelona, Catalonia, Spain

(*Received November* 27, 1996; *accepted in revised form July* 28, 1997)

Abstract—The South China Sea, due to its location and high sedimentary C_{37} alkenone concentrations, is an ideal environment for the evaluation of the linear relationship between the alkenone-derived U^k_{37} index and sea surface temperatures (SST) at the warm boundary. The alkenone compounds in this system have been analyzed in a series of coretop sediments covering most of the areas situated far from the influence of riverine inputs. The resulting U^k_{37} indices have been correlated with averaged SST of various depth levels and seasons. Curve fitting of these parameters have shown that the linear U^k_{37}/SST relationship is maintained at the warm end, which strongly contrasts with the lack of correlation at low SST reported in other studies. The best curve fittings of the U^k_{37} measurements are obtained for the annually averaged 0–30 m water column temperatures, providing a linear equation, $U^k_{37} = 0.031T + 0.092$, that is the same within error limits as those previously obtained in open ocean sites or *Emiliania huxleyi* cultures. *Copyright © 1997 Elsevier Science Ltd*

1. INTRODUCTION

The long chain C_{37}-C_{39} alkenones are sedimentary compounds whose only known sources are Haptophyceae algae (Volkman et al, 1980; Marlowe et al., 1984). These compounds are used for past sea surface temperature (SST) estimations in open marine systems. The relationship between ketone composition and water temperature is based on the degree of unsaturation of the ketone distributions which is measured by means of several indices.

The first index was defined by Brassell et al. (1986a,b) as

$$U^k_{37} = (C_{37:2} - C_{37:4})/(C_{37:2} + C_{37:3} + C_{37:4})$$

where $C_{37:4}$, $C_{37:3}$, and $C_{37:2}$ are the concentrations of heptatriaconta-(8E,15E,22E,29E)-tetraen-2-one, heptatriaconta-(8E, 15E,22E)-trien-2-one, and heptatriaconta-(15E,22E)-dien-2-one, respectively. However, the low concentrations of the tetraunsaturated ketone encountered in the sediments (Brassell et al, 1986a) led to propose a simplified expression (Prahl and Wakeham, 1987):

$$U^{k'}_{37} = C_{37:2} / (C_{37:2} + C_{37:3})$$

The first evidence of a link between U^k_{37} indices and SST was provided by comparison of a U^k_{37} profile and the $\delta^{18}O$ composition of foraminiferal species in an Atlantic Ocean sediment core encompassing the last 120.000 years (Brassell et al, 1986a). Later, U^k_{37} determinations in isothermally cultured *Emiliania huxleyi*, the most abundant coccolithophorid species in the present oceans (Marlowe et al., 1984), showed that the relationship was linear in a range of 8–25°C (Prahl and Wakeham, 1987; Prahl et al, 1988).

This linear relationship was confirmed in subsequent studies encompassing water column particulate organic matter (Prahl and Wakeham, 1987; Prahl et al., 1988, 1993; Conte et al., 1992; Freeman and Wakeham, 1992; Conte and Eglinton, 1993; Sikes and Volkman, 1993; Ternois et al., 1997) and coretop sediments (Prahl et al., 1988, 1993; McCaffrey et al., 1990; Sikes et al, 1991; Kennedy and Brassell, 1992; Conte et al, 1992; Rosell-Melé et al., 1995; Madureira et al, 1995; Sonzogni et al., 1997). In this latter case, the U^k_{37} determinations were compared with average SST of the overlying waters.

On these grounds, one important aspect to be considered concerns the cold and warm limits of the U^k_{37} - SST linear relationship. Whereas the cold temperatures (−0.7–12.2°C) have been examined in one previous study (Sikes and Volkman, 1993), the linear range at the warm boundary (>25°C) is still pending to be evaluated. This aspect is important because average temperatures in the order of 25–29°C are encountered in many warm oceans (Table 1). These temperatures are located at low latitudes and play an important role in the atmosphere-ocean interaction, conditioning the position of the Intertropical Convergence Zone. Thus, the use of the U^k_{37} index to reconstruct paleo SST in the warm areas can be crucial to study changes in the intensity of the Trade Winds and the Hadley circulation.

The South China Sea is a tropical sea amongst the warmest in the Earth (Table 1). Its warm SST together with its high amounts of sedimentary C_{37} alkenones make it an ideal site to evaluate the linearity of U^k_{37} vs. SST at the warm end. Furthermore, SST paleoreconstruction in this area is of great interest to monitor changes in monsoonal activity and thus in global circulation.

Accordingly, this work is aimed to evaluate the applicability of the U^k_{37} index as paleothermometer in the South China Sea, which is taken as reference area for the warm SST boundary. The study has been performed by analysis of a series of thirty-one top cores distributed throughout the areas free from coastal influence (Fig.1). The U^k_{37} indices of the sedimentary C_{37} alkenone distributions have been compared with the modern SST corresponding to different water depths and seasons available from oceanographic databases (Levitus, 1994). The results have been evaluated in terms of the oceanographic significance of the seasonal and depth profile patterns reflected in the correlations.

Table 1. Main warm water areas in the world oceans and seas and aproximate annual SST range (Levitus, 1994).

Warm Marine Areas	Surface waters temperature range (°C)
Equatorial Atlantic	25–28
Caribbean Gulf	25–29.5
Micronesia area	25–29.5
Arabian Gulf	28–29.5
Sulu Sea	26.5–30.5
South China Sea	23–29

2. MATERIALS AND METHODS

The sediment samples studied correspond to the upper centimeter (0–1 cm) of a box-core set obtained during the R/V SONNE cruise in April–June 1994 (Sarnthein et al., 1994; Fig. 1). The sedimentation rates of these cores range between 5 and 50 cm/ky (M. Sarnthein, pers. commun.). Thus, the upper sediment sections average approximately among 20 and 200 y, not taking into account bioturbation. If a 10 cm thickness of bioturbated sediment is considered (Berger and Heath, 1968; Thomson et al., 1995), the sections used for this study would average 2000 years at the most. Since the latter Holocene temperatures are not believed to have changed significantly, comparison of $U^{k'}_{37}$ data with the modern SST of the overlying surface waters is a consistent approximation. The water depths of these cores range between 900 and 4200 m.

The procedures and equipment used for the $U^{k'}_{37}$ index determinations are described elsewhere (Villanueva et al., 1997). Briefly, sediment samples were freeze-dried and manually grounded for homogeneity. After addition of an internal standard of nonadecan-1-ol, hexatriacontane, and tetracontane, approximately 3 g of dry sediment were extracted in an ultrasonic bath with dichloromethane, and the extracts were hydrolyzed with 6% potassium hydroxide in methanol to eliminate wax ester interferences. After derivatizing with bis(trimethylsilyl)trifluoroacetamide, the extracts were analyzed by gas chromatography coupled to flame ionization detection. Selected samples were examined by gas chromatography coupled to mass spectrometry to confirm compound identification and check for possible coelutions.

Modern SST data for comparison with $U^{k'}_{37}$ values has been triangle interpolated for each South China Sea station from the one-degree latitude-longitude grid World Ocean Atlas 1994 data set (Levitus, 1994). The World Ocean Atlas 1994 and the atlas data sets were produced by the National Oceanographic Data Center (NODC) Ocean

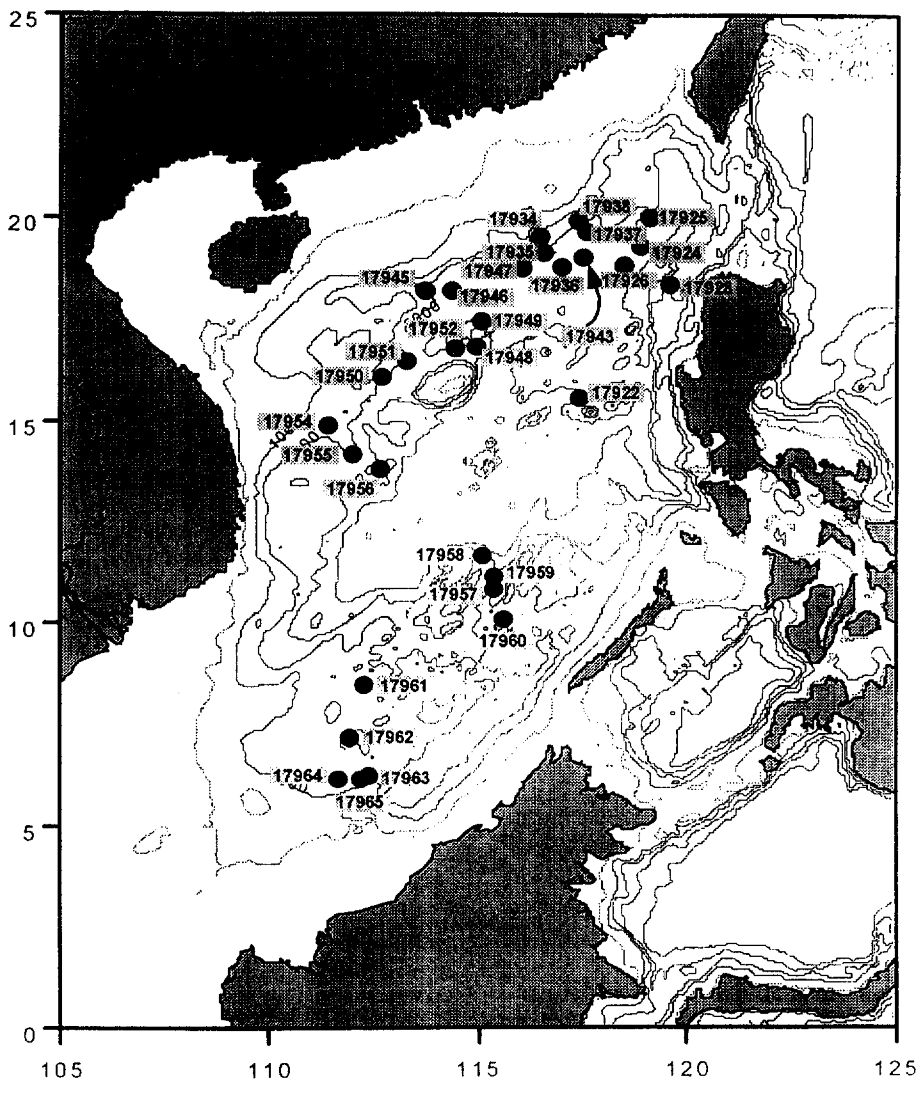

Fig. 1. Map of the sample locations in the South China Sea. The sediment samples collected for study correspond to the upper centimeter (0–1cm) of box-cores obtained during the R/V SONNE cruise in April–June 1994.

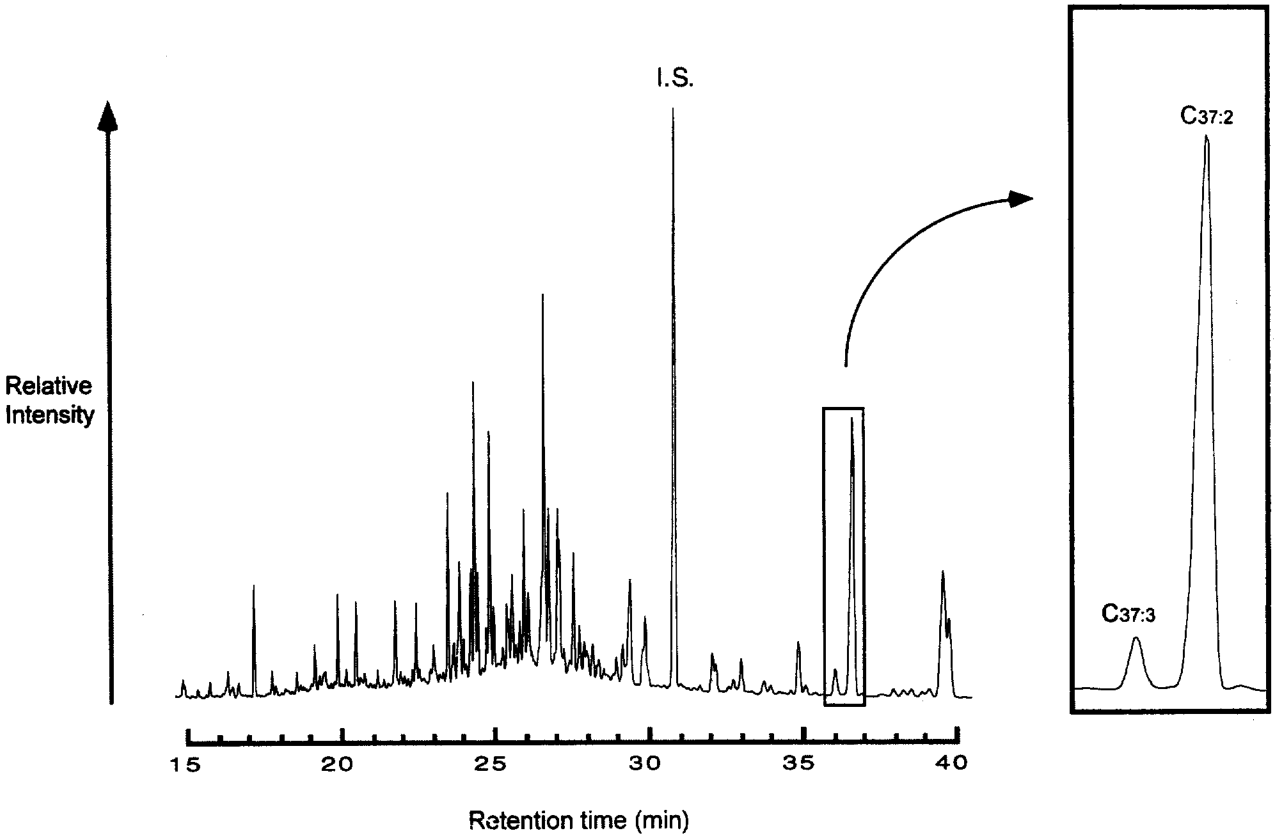

Fig. 2. Representative chromatogram of the South China Sea coretop samples (17943). $C_{37:3}$: heptatriaconta-(8E,15E,22E)-trien-2-one. $C_{37:2}$: heptatriaconta-(15E,22E)-dien-2-one. I.S. Internal Standard (hexatriacontane).

Climate Laboratory using NODC's data holdings as of the first quarter of 1993, which includes global distribution maps of the data representing approximately the last hundred years (Levitus, 1982). World Ocean Atlas 1994 database is quality controlled through procedures documented in two NOAA Technical Reports (Boyer and Levitus, 1994; Conkright et al., 1994). Data for water temperature at the standard depths of 0, 10, 20, 30, and 50 m is available from this data set. Also, season composite temperatures are available based on seasons following the Northern Hemisphere convention. Some authors have noted that Levitus data can be smoothed away for small-scale plumes of low salinity surface water in areas influenced by fluvial freshwater inputs (Wang et al., 1995). For this reason, the coretop selection chosen for this study has not included samples from the coastal western areas influenced by major river discharges.

3. RESULTS AND DISCUSSION

3.1. C_{37} Alkenone Composition

A representative chromatogram of the C_{37} alkenone composition in the superficial sediments of the South China Sea is shown in Fig. 2. No $C_{37:4}$ is found in these warm waters. Thus, the above described U^{k}_{37} and $U^{k'}_{37}$ indices are identical. In fact, in such warm waters, the U^{k}_{37} and $U^{k'}37$ values are close to one, which means that the concentrations of $C_{37:3}$ are low. In these conditions, the total concentrations of C_{37} alkenones must be high for the accurate measurement of the concentration of this triunsaturated species. In the sediments considered for this study, the total C_{37} alkenone abundances range between 200 and 1000 ng/g and the U^{k}_{37} indices between 0.910 and 0.972. The highest U^{k}_{37} index, 0.972, (lowest relative proportion of $C_{37:3}$) is found in samples with total C_{37} alkenone abundance of about 500 ng/g, which corresponds to a $C_{37:3}$ concentration of 15 ng/g. This minimal concentration is sufficient for GC injection of amounts above the irreversible adsorption threshold which biases the U^{k}_{37} determination upon alkenone analysis with wall coated capillary columns (Villanueva and Grimalt, 1996).

Another distinct aspect of the alkenone composition in warm waters is the absence of C_{36} alkenoates which are found at temperatures colder than 24°C (Conte et al., 1992). These compounds, particularly the methylhexatriaconta-7E,14E,21E-trienoate, coelute with the C_{37} alkenones difficulting the U^{k}_{37} measurements. In any case, the potential interference of this compound and other waxes is eliminated with the hydrolysis step included in the analytical procedure of these South China Sea sediments (Villanueva et al., 1996).

3.2. U^{k}_{37} Measurements and the Vertical Temperature Profile

As common sense suggests, the sedimentary U^{k}_{37} should mainly represent the seawater properties of the seasons and depths of higher Haptophytae development (Conte et al., 1992; Brassell, 1993; Chapman et al., 1996). Increased production leads to higher sinking of detritus (Lampitt, 1985) and reduces the residence time in the water column, which further enhances preservation (Conte et al., 1992).

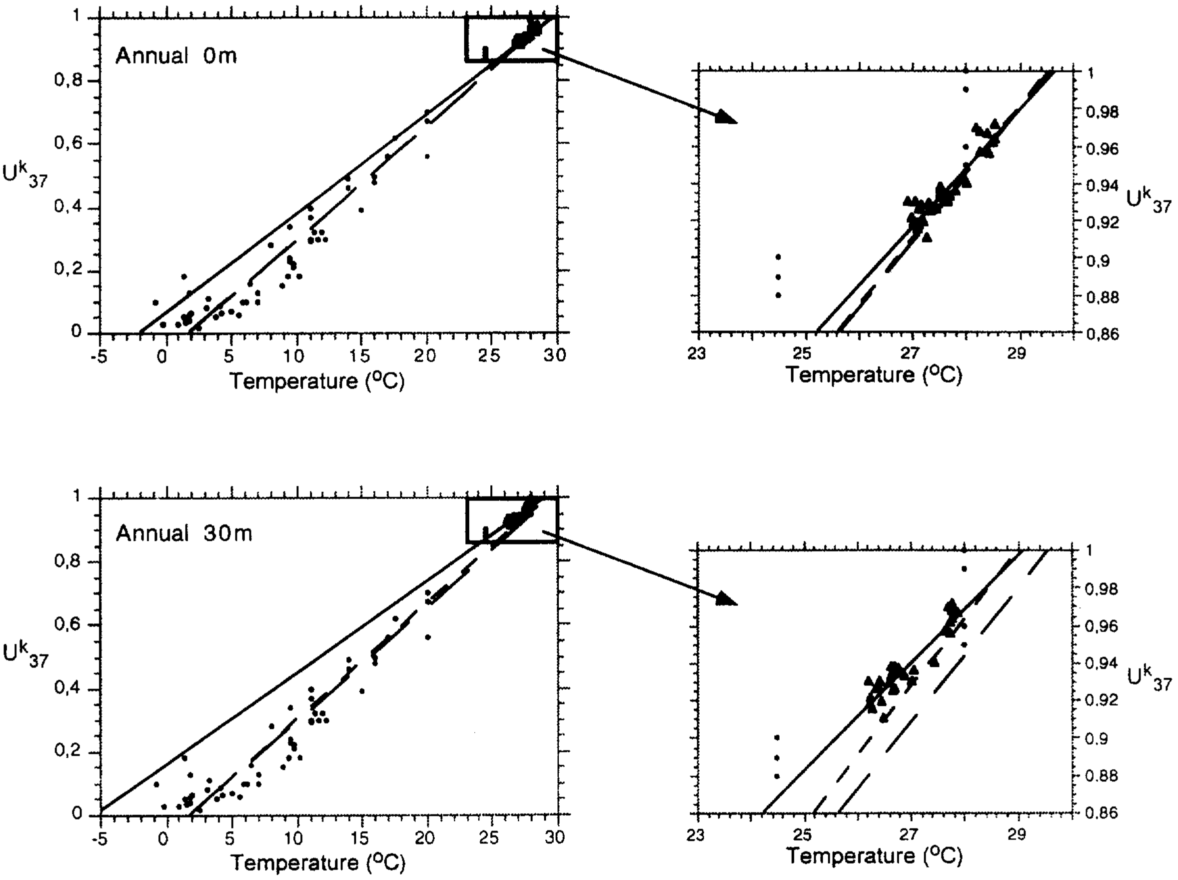

Fig. 3. In triangles, U^k_{37} index for the South China Sea sediments shown in Fig. 1. These are represented vs. the modern times annual average SST overlying the coretop locations at different depths (0, 30, 50 m and average 0–30 m; Levitus, 1994). In circles, previous reported data for particulate and sediment trap matter (Prahl and Wakeham, 1987; Sikes and Volkman, 1993), corresponding to a large series of oceanic sites. Three linear regression curves are shown: (1) only particulate and sediment trap matter from the previously reported data over a temperature span of −0.7–28°C, (2) only the South China Sea data, (3) all pooled data.

Unfortunately, the information on the annual coccolithophorid production patterns in the South China Sea is very limited. In this respect, one recent sediment trap study on coccolithophorid sinking fluxes (Wiesner et al., 1996), has not evidenced any specific seasonal period of maximal productivity. Likewise, no information is available on productivity differences in subsurface waters.

In the absence of sufficient knowledge on the dynamics of the Haptophyta populations in the South China Sea waters, any calibration study must consider both the yearly temperature cycle and the various depths at which Haptophyta are encountered. It is well known that Haptophyta live within the euphotic zone, not being restricted to the sea surface (Okada and Honjo, 1973; Okada and McIntyre, 1979). *E. huxleyi*, the main alkenone producer in the present times, synthesizes a carotenoid pigment, 19'hexanoyloxyfucoxanthin (Haxo, 1985), that enables to do the photosynthesis at the bottom of the subsurface chlorophyll maximum, where nutrients are often replete (Prahl et al., 1993). Accordingly, in a first comparison we have correlated the sedimentary U^k_{37} data set with the annual averaged SST overlying the coretop locations at various water depths (0, 10, 20, 30, and 50 m).

As shown in Fig. 3, the U^k_{37} index and annual averaged SST exhibit a remarkable linearity at all depths. The correlations involve temperature ranges between 27–29°C and 24.5–26.5°C, corresponding to a 0 and 50 m depth, respectively. All linear correlation coefficients (R) are higher than 0.9, with the best fit for 30 m depth (R=0.932; Table 2). The lowest R value, 0.909, corresponds to the deeper section (50 m). Statistical F tests between variance residuals at a significance level of 95% do not show significant differences between these correlation coefficients, which corresponds to similar 0–50 m depth-temperature gradients in all studied sites. As expected, the water column temperature profiles are essentially differentiated by the shifting effect of local SST. However, there is a slight trend towards worse linear correlations below 30 m depth. This trend has also been reported in closely related studies performed in other areas (Rosell-Melé et al., 1995; Sonzogni et al., 1997).

The slopes of these correlations range between 0.025 and 0.032, the latter being a value close to the slope of the linear equation taken as reference in many studies (Prahl and Wakeham, 1987). The temperatures exhibiting the more deviated values (lowest slope, 0.025) are those corresponding to the lowest depth, 50 m.

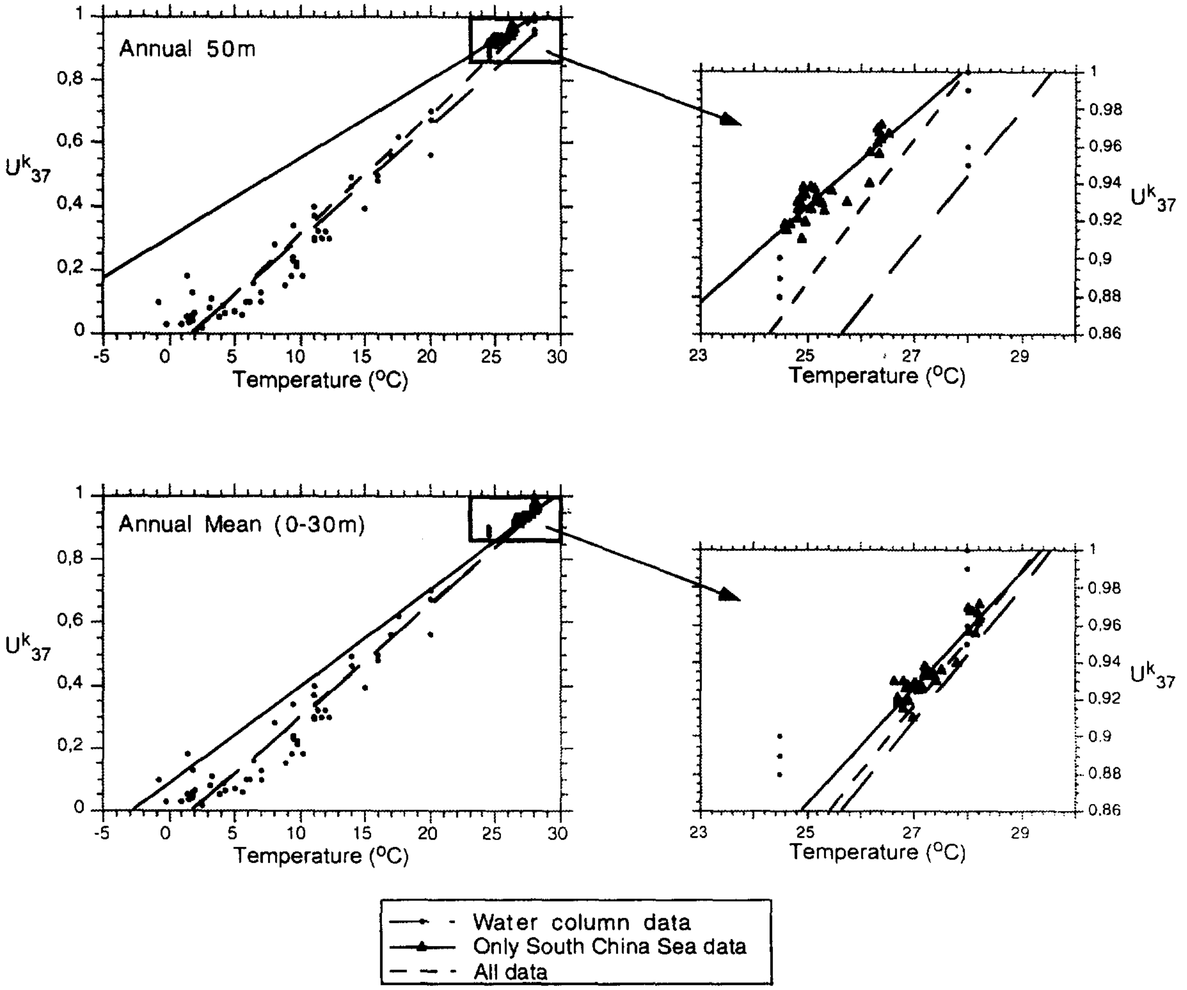

Fig. 3. (Continued)

The similarity of these slopes with those from previously calibrated U^k_{37}/SST linear equations and the high R values are very remarkable in view of the narrow temperature range recorded in the South China Sea. The linear correlation between U^k_{37} and SST is, therefore, proved to work in the warm boundary (up to 29°C), which represents a distinct feature from the observed lack of linearity in the cold extreme of the calibration curve (Sikes and Volkman, 1993).

The comparison of these sedimentary values to U^k_{37}/SST data from water column measurements provide further ground on the reliability of the sedimentary estimates since water column data correspond to direct temperature determi-

Table 2. Parameters of the linear regression curves between annually averaged SST at different depth levels (Levitus, 1994) and the South China Sea U^k_{37} data or the combined South China Sea and particulate and sediment trap U^k_{37} data reported elsewhere (Prahl and Wakeham, 1987; Sikes and Volkman, 1993).

Depth		Only South China Sea data	All data	Depth		Only South China Sea data	All data
0 m	temperature range	26.9 − 28.6 = 1.7	−0.7 − 28.6 = 29.3	30 m	temperature range	26.2 − 27.9 = 1.7	−0.7 − 28.0 = 28.7
	y-intercept (a)	0.070 ± 0.142	−0.054 ± 0.022		y-intercept (a)	0.162 ± 0.114	−0.059 ± 0.023
	slope (b)	0.031 ± 0.005	0.036 ± 0.001		slope (b)	0.029 ± 0.004	0.037 ± 0.001
	correlation coefficient (R)	0.918	0.989		correlation coefficient (R)	0.932	0.989
	correlation coefficient (R^2)	0.843	0.978		correlation coefficient (R^2)	0.869	0.978
10 m	temperature range	26.9 − 28.4 = 1.5	−0.7 − 28.4 = 29.1	50 m	temperature range	24.6 − 26.5 = 1.9	−0.7 − 28.0 = 28.7
	y-intercept (a)	0.046 ± 0.146	−0.054 ± 0.022		y-intercept (a)	0.030 ± 0.111	−0.069 ± 0.026
	slope (b)	0.032 ± 0.005	0.036 ± 0.001		slope (b)	0.025 ± 0.004	0.039 ± 0.001
	correlation coefficient (R)	0.919	0.989		correlation coefficient (R)	0.909	0.986
	correlation coefficient (R^2)	0.845	0.978		correlation coefficient (R^2)	0.826	0.972
20 m	temperature range	26.7 − 28.2 = 1.5	−0.7 − 28.2 = 28.9	Mean (0–30)	temperature range	26.7 − 28.2 = 1.5	−0.7 − 28.2 = 28.9
	y-intercept (a)	0.098 ± 0.131	−0.056 ± 0.022		y-intercept (a)	0.092 ± 0.131	−0.056 ± 0.022
	slope (b)	0.031 ± 0.005	0.036 ± 0.001		slope (b)	0.031 ± 0.005	0.036 ± 0.001
	correlation coefficient (R)	0.926	0.989		correlation coefficient (R)	0.926	0.989
	correlation coefficient (R^2)	0.857	0.978		correlation coefficient (R^2)	0.858	0.978

Table 3. Parameters of the linear regression curves between SST at 0–30 m and different seasons (Levitus, 1994) and the South China Sea $U^{k'}_{37}$ data or the combined South China Sea and particulate and sediment trap $U^{k'}_{37}$ data reported elsewhere (Prahl and Wakeham, 1987; Sikes and Volkman, 1993).

Season		Only South China Sea data	All data
Winter	temperature range	23.9 − 27.1 = 3.2	−0.7 − 28.0 = 28.7
	y-intercept (a)	0.573 ± 0.052	0.067 ± 0.027
	slope (b)	0.014 ± 0.002	0.038 ± 0.001
	correlation coefficient (R)	0.937	0.985
	correlation coefficient (R^2)	0.878	0.970
Spring	temperature range	27.2 − 29.0 = 1.8	−0.7 − 29.0 = 29.7
	y-intercept (a)	0.093 ± 0.156	−0.050 ± 0.022
	slope (b)	0.030 ± 0.006	0.035 ± 0.001
	correlation coefficient (R)	0.899	0.989
	correlation coefficient (R^2)	0.808	0.978
Summer	temperature range	28.2 − 29.0 = 0.8	−0.7 − 29.0 = 29.7
	y-intercept (a)	0.436 ± 1.058	−0.045 ± 0.022
	slope (b)	0.175 ± 0.037	0.035 ± 0.001
	correlation coefficient (R)	0.034	0.989
	correlation coefficient (R^2)	0.001	0.978
Autumn	temperature range	26.4 − 28.3 = 1.9	−0.7 − 28.3 = 29.0
	y-intercept (a)	0.192 ± 0.100	−0.057 ± 0.022
	slope (b)	0.027 ± 0.004	0.036 ± 0.001
	correlation coefficient (R)	0.943	0.989
	correlation coefficient (R^2)	0.889	0.978

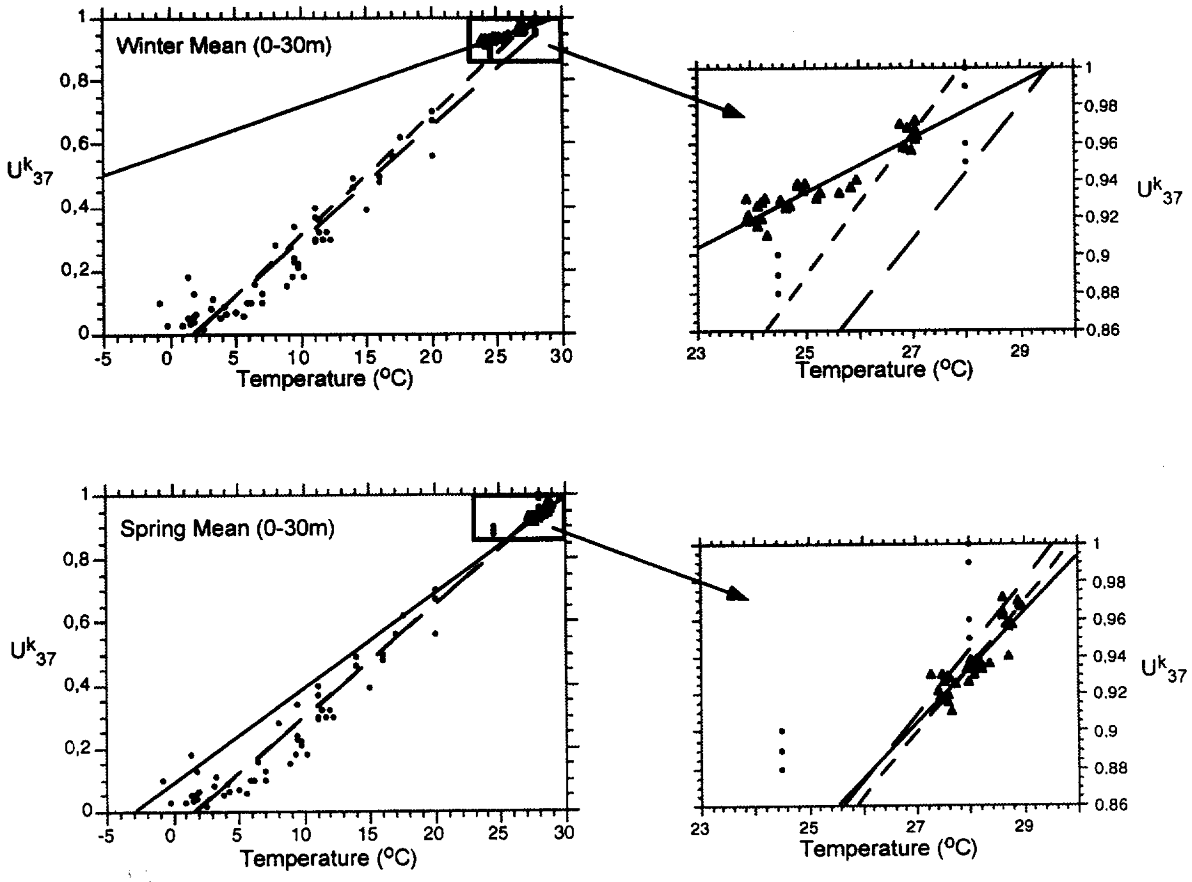

Fig. 4. In triangles, $U^{k'}_{37}$ index for the South China Sea sediments shown in Fig. 1. They are represented vs. the modern times 0–30 m water depth temperatures overlying the coretop locations at different seasons (Levitus, 1994). In circles, previous reported data for particulate and sediment trap matter (Prahl and Wakeham, 1987; Sikes and Volkman, 1993), corresponding to a large series of oceanic sites. Three linear regression curves are shown: (1) only particulate and sediment trap matter from the previously reported data over a temperature span of −0.7–28°C, (2) only the South China Sea data, (3) all pooled data.

nations in the sites of alkenone production (Sikes et al., 1997). For this purpose, the South China database has been pooled with previously reported data from particulate and sediment trap material encompassing the whole range of temperatures (−0.7–28°C) obtained from the study of a large variety of oceanic sites (Northeast Pacific, Caribbean Sea, North Atlantic, Equatorial Pacific, and Southern Ocean; Prahl and Wakeham, 1987; Sikes and Volkman, 1993).

The joint correlation of both series shows that the linear relationship is maintained irrespectively of the water depth temperatures assigned to the South China Sea sedimentary U^{k}_{37} values (Fig. 3). However, the lowest R coefficient and highest deviation between slopes of the South China Sea series and combined data set corresponds to the assignment of the sedimentary U^{k}_{37} values to the 50 m depth temperatures. In contrast, no major differences are observed between the slopes obtained by assignment of the South China Sea U^{k}_{37} values to the temperatures of 0, 10, 20, or 30 m depths. These depths also correspond to the highest R coefficients. In these conditions, taking into consideration the water column habitat of the Haptophyceae algae, the most reasonable estimate corresponds to the calibration with the averaged water column temperatures in the 0–30 m depth range.

3.3. U^{k}_{37} and Seasonality

As indicated above, the scarce information available on the seasonal productivity patterns of Haptophyceae algae in the South China Sea points to diverse periods of increased production distributed throughout the year (Wiesner et al., 1996). Nevertheless, it is interesting to evaluate whether the South China Sea U^{k}_{37} data exhibit a seasonal pattern.

The calculation of the averaged 0–30 m depth temperatures along the four seasonal periods area (Levitus, 1994) shows that seasonality in the South China Sea (Table 3) involves a geographic temperature distribution over very different ranges. The temperature range is widest in winter (3.2°C), intermediate in spring and autumn (1.8–1.9°C) and narrowest in summer (only 0.8°C). Thus, the South China Sea is practically homogeneous during summer. The small temperature differences of this season are difficult to distinguish with the U^{k}_{37} index because stringent analytical requirements are needed to decrease the estimated error below ± 0.5°C (Villanueva and Grimalt, 1996, 1997).

The correlation of the South China Sea U^{k}_{37} data with these temperatures shows high R values for the winter,

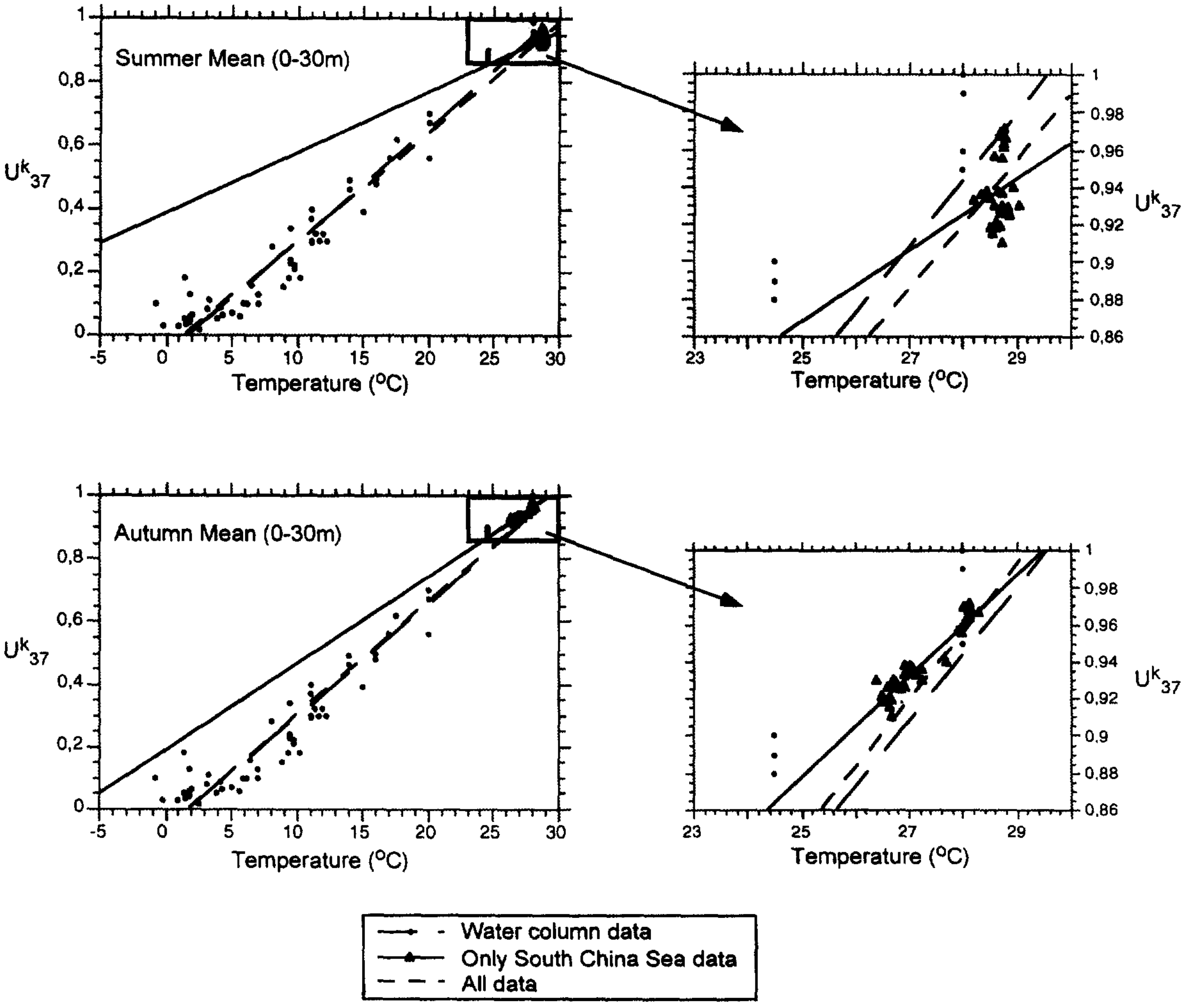

Fig. 4. (Continued)

spring, and autumn periods (Table 3) corresponding to linear $U^{k'}_{37}$/SST relationships (Fig. 4). As expected, the wider the temperature range, the more correlated are the values. In summer, the extremely low temperature range does not allow for a proper linear regression to be established.

The consistency of these seasonal series with the above mentioned data from suspended particles and sediment traps (Prahl and Wakeham, 1987; Sikes and Volkman, 1993) has also been evaluated by linear regression of all pooled values and comparison of the resulting slopes and correlation coefficients (Table 3 and Fig. 4). As shown in Fig. 4, the "temperature point" generated by representation of the South China Sea $U^{k'}_{37}$ data vs. summer SST is in agreement with the straight line defined by the corresponding sediment trap and suspended particulate data. However, the slopes derived from linear regression of seasonally-grouped $U^{k'}_{37}$/SST South China Sea data or pooled South China Sea and water particulate data show more discrepancies than in the case of the annual averages. In this respect, it is worth noticing that the highest similarities between the two data sets correspond to two noncorrelative seasons, spring and autumn. These results are consistent with the lack of a defined annual period for maximal Haptophyta growth in the South China Sea (Wiesner et al., 1996), and suggest that the best $U^{k'}_{37}$/SST equation corresponds to the averaged annual temperatures. The complete database corresponding to these points is reported in Table 4.

3.4. Calibration Equations

Since the best calibration conditions for the South China Sea coretop sedimentary $U^{k'}_{37}$ data corresponds to water column temperatures annually averaged over the top 0–30 m, the equation $U^{k'}_{37} = 0.031T + 0.092$ is obtained as specific relationship for the South China Sea. This equation is almost the same as that found in a sediment calibration based on a large series of open ocean sites ($U^{k'}_{37} = 0.031T + 0.082$; Sikes et al., 1991). The authors of this calibration concluded that theirs was identical within the error limits to the equation obtained from *E. huxleyi* cultures by Prahl and Wakeham (1987) $U^{k'}_{37} = 0.033T + 0.043$. In fact, within the temperature range of interest in the area of study, 24–29°C, the maximum difference between the equation obtained in the present work and that of Prahl and Wakeham (1987) is 0.3°C. This difference is negligible when compared with the analytical error threshold of the $U^{k'}_{37}$ determinations, 0.5°C (Villanueva and Grimalt, 1996; Villanueva et al, 1997).

4. CONCLUSIONS

The $U^{k'}_{37}$ index is a useful paleothermometer in the warm end of the SST encountered in open marine systems. The calibration performed in the South China Sea shows a linear relationship between $U^{k'}_{37}$ and SST. The best linear fittings correspond to the annually averaged water column temperatures between 0 and 30 m. Curve fitting of the alkenone measurements to these SST values gives rise to a linear equation, $U^{k'}_{37} = 0.031T + 0.092$, that is the same within error limits as those reported for a large series of ocean sites (Sikes et al., 1991) and *E. huxleyi* cultures (Prahl and Wakeham, 1987). The $U^{k'}_{37}$ index can, therefore, be used to estimate past SST in the warm waters commonly found in low latitude oceans and seas.

Table 4. $U^{k'}_{37}$ data for the samples studied in this work and modern times annually average temperatures (°C) at 0–30 m depth. (Levitus, 1994).

Station	Longitude	Latitude	$U^{k'}_{37}$	Annual temperature (°C) (0–30 m)
17922	117.46	15.42	0.940	27.81
17924	118.85	19.41	0.929	27.04
17925	119.05	19.85	0.930	26.83
17926	118.73	19.00	0.925	27.10
17928	119.75	18.27	0.930	27.42
17934	116.46	19.03	0.918	26.73
17935	116.53	18.88	0.926	26.85
17936	117.12	18.77	0.928	26.89
17937	117.67	19.50	0.921	26.71
17938	117.54	19.79	0.930	26.66
17943	117.55	18.95	0.920	26.92
17945	113.78	18.13	0.918	26.80
17946	114.25	18.13	0.915	26.82
17947	116.03	18.47	0.910	26.99
17948	114.90	16.71	0.937	27.26
17949	115.17	17.35	0.927	27.19
17950	112.90	16.09	0.938	27.20
17951	113.41	16.29	0.934	27.21
17952	114.47	16.67	0.938	27.22
17954	111.53	14.80	0.933	27.23
17955	112.18	14.12	0.933	27.40
17956	112.59	13.85	0.936	27.54
17957	115.30	10.90	0.968	28.08
17958	115.08	11.62	0.969	28.01
17959	115.29	11.14	0.968	28.07
17960	115.56	10.12	0.966	28.20
17961	112.33	8.51	0.956	28.03
17962	112.08	7.18	0.956	28.17
17963	112.67	6.17	0.963	28.24
17964	112.21	6.16	0.961	28.21
17965	112.55	6.16	0.972	28.24

Acknowledgments—We thank Prof. M. Sarnthein (University of Kiel) for his useful comments and kind access to South China Sea sediments. We also thank Drs. M. C. Herrero (University of Salamanca) for valuable help in the statistic data processing and U. Pflaumann (University of Kiel) for assistance in Levitus data interpolations. We are grateful to E. Bard and an anonymous reviewer for their interesting indications. CP thanks a Ph.D grant from C.I.R.I.T. (Generalitat de Catalunya). This work was in part financed by the European Union (Human and Capital Mobility Contract No. CHRX-CT94-0424). The samples included in this study were collected during a R/V SONNE cruise.

REFERENCES

Berger W. H. and Heath G. R. (1968) Vertical mixing in pelagic sediments. *J. Mar. Res.* **26**, 134–143

Boyer T. P. and Levitus S. (1994) Quality control and processing of historical temperature, salinity, and oxygen data. NOAA Tech. Rept. NESDIS 81.

Brassell S. C. (1993) Applications of biomarkers for delineating marine palaeoclimatic fluctuations during the Pleistocene. In *Organic Geochemistry: Principles and Applications* (ed. M. H. Engel and S. A. Macko), pp. 699–738. Plenum Press.

Brassell S. C., Eglinton G., Marlowe I. T., Pflaumann U., and Sarnthein M. (1986a) Molecular stratigraphy: A new tool for climatic assessment. *Nature* **320**, 129–133

Brassell S. C. et al. (1986b) Palaeoclimatic signals recognized by

chemometric treatment of molecular stratigraphic data. *Org. Geochem.* **10**, 649–660
Chapman M. R., Shackleton N. J., Zhao M., and Eglinton G. (1996) Faunal and alkenone reconstructions of subtropical North Atlantic surface hydrography and paleotemperature over tha last 28 kyr. *Paleoceanography* **11**, 343–357
Conte M. H.and Eglinton G. (1993) Alkenone and alkenoate distributions within the euphotic zone of eastern north Atlantic: Correlation with production temperature. *Deep-Sea Res.* **40**, 1935–1961
Conte M. H., Eglinton G., and Madureira L. A. S. (1992) Long-chain alkenones and alkyl alkenoates as palaeotemperature indicators: their production, flux and early sedimentary diagenesis in the eastern North Atlantic. *Org. Geochem.* **19**, 287–298
Conkright M. E., Boyer T. P., and Levitus S. (1994) Quality control and processing of historical nutrient data. NOAA Tech. Rept. NESDIS 79.
Freeman K. H. and Wakeham S. G. (1992) Variations in the distributions and isotopic compositions of alkenones in Black Sea particles and sediments. *Org. Geochem.* **19**, 277–285
Haxo F. T. (1985) Photosynthetic action spectrum of the coccolithophorid, *Emiliania huxleyi* (Haptophyceae): 19'hexanoyloxyfucoxanthin as antenna pigment. *J. Phycol.* **21**, 282–287.
Kennedy J. A. and Brassell S. C. (1992) Molecular records of twentieth-century El Niño events in laminated sediments from the Santa Barbara basin. *Nature* **357**, 62–64
Lampitt R. S. (1985) Evidence for the seasonal deposition of detritus to the deep-sea floor (Porcupine Bight, N.E. Atlantic) and its subsequent resuspension. *Deep-Sea Res.* **32**, 885–897
Levitus S. (1982) *Climatological Atlas of the World Ocean*. US Dept. Commerce.
Levitus S. (1994) *World Ocean Atlas*. NOAA NESDIS. US Govt. Print. Office.
Madureira L. A. S., Conte M. H., and Eglinton G. (1995) Early diagenesis of lipid biomarker compounds in North Atlantic sediments. *Paleoceanography* **10**, 627–642
McCaffrey M. A., Farrington J. W., and Repeta D. T. (1990) The organic geochemistry of Peru margin surface sediments: I. A comparison of the C_{37} alkenone and historical El Niño records. *Geochim. Cosmochim. Acta* **54**, 1671–1682.
Marlowe I. T., Green J. C., Neal A. C., Brassell S. C., Eglinton G., and Course P. A. (1984) Long-chain (n-C_{37}-C_{39}) alkenones in the Prymnesiophyceae. Distribution of alkenones and other lipids and their taxonomic significance. *Br. Phycol. J.* **19**, 203–216
Okada H. and Honjo S. (1973) The distribution of oceanic coccolithophorids in the Pacific. *Deep-Sea Res.* **20**, 355–374
Okada H. and McIntyre A. (1979) Seasonal distribution of modern coccolithophores in the Weastern North Atlantic Ocean. *Mar. Biol. Berlin* **54**, 319–328
Prahl F. G. and Wakeham S. G. (1987) Calibration of unsaturation patterns in long-chain ketone composition for paleotemperature assessment. *Nature* **330**, 367–369
Prahl F. G., Muelhausen L. A., and Zahnle D. A. (1988) Further evaluation of long-chain alkenones as indicators of paleoceanographic conditions. *Geochim. Cosmochim. Acta* **52**, 2303–2310.
Prahl F. G., Collier R. B., Dymond J., Lyle M., and Sparrow M. A. (1993) A biomarker perspective on prymnesiophyte productivity in the northeast Pacific Ocean. *Deep-Sea Res.* **40**, 2061–2076
Rosell-Melé A., Eglinton G., Pflaumann U., and Sarnthein M. (1995) Atlantic coretop calibration of the U^{k}_{37} index as sea-surface paleotemperature indicator. *Geochim. Cosmochim. Acta* **59**, 3009–3107
Sarnthein M., Pflaumann U., Wang P. X., and Wong H. K. (eds.) (1994) Preliminary report on Sonne-95 cruise Monitor Monsoon to the South China Sea. *Ber.-Rep., Geol.-Paläontol. Inst.Univ.Kiel* **68**, 1–225
Sikes E. L. and Volkman J. K. (1993) Calibration of alkenone unsaturation ratios ($U^{k'}_{37}$) for paleotemperature estimation in cold polar waters. *Geochim. Cosmochim. Acta* **57**, 1883–1889
Sikes E. L., Farrington J. W., and Keigwin L. D. (1991) Use of the alkenone unsaturation ratio U^{k}_{37} to determine past sea surface temperatures: Coretop SST calibrations and methodology considerations. *Earth Planet. Sci. Lett.* **104**, 36–47
Sikes E. L., Volkman J. K., Robertson L. G., and Pichon J.-J. (1997) Alkenones and alkenes in surface waters and sediments of the Southern Ocean: Implications for paleotemperature estimation in polar regions. *Geochim. Cosmochim. Acta* **61**, 1495–1505.
Sonzogni C., Bard E., Rostek F., and Dollfus D. (1997) Temperature and salinity effects on alkenone ratios measured in surface sediments from the Indian Ocean. *Quat. Res.* **47**, 344–355
Ternois Y., Sicre M.-A., Boireau A., Conte H. H., and Eglinton G. (1997) Evaluation of long-chain alkenones as paleo-temperature indicators in the Mediterranean Sea. *Deep-Sea Res.* **44**, 271-286.
Thomson J., Colley S., Anderson R., Cook G. T., and MacKenzie A. B. (1995) A comparison of sediment accumulation chronologies by the radiocarbon and $^{230}Th_{excess}$ methods. *Earth Planet. Sci. Lett.* **133**, 59-70
Villanueva J. and Grimalt J. (1996) Pitfalls in the chromatographic determination of the alkenone U^{k}_{37} index for paleotemperature estimation. *J. Chrom.* **723**, 285-291
Villanueva J. and Grimalt J. (1997) Gas chromatographic tuning of the $U^{k'}_{37}$ paleothermometer. *Anal. Chem.* **69**, 3329–3332.
Villanueva J., Pelejero C., and Grimalt J. (1997) Clean-up procedures for the unbiased estimation of C_{37} alkenone sea surface temperatures and terrigenous n-alkane inputs in paleoceanography. *J. Chrom.* **757**, 145–151.
Volkman J. K., Eglinton G., Corner E. D. S., and Sargent J. R. (1980) Novel unsaturated straight-chain C_{37}-C_{39} methyl and ethyl ketones in marine sediments and a coccolithophore *Emiliania huxleyi*. In *Advances in Organic Geochemistry 1979* (ed. A. G. Douglas and J. R. Maxwell), pp. 219–227. Pergamon Press.
Wang L., Sarnthein M., Duplessy J-C., Erlenkeuser H., Jung S., and Pflaumann U. (1995) Paleo sea surface salinities in the low-latitude Atlantic: The $\delta^{18}O$ record of *Globigerinoides ruber* (white). *Paleoceanography* **10**, 749–761
Wiesner M. G., Zheng L., Wong H. K., Wang Y., and Chen W. (1996) Fluxes of particulate matter in the South China Sea. In *Particle Flux in the Ocean* (ed V. Ittekkot et al.), pp. 293–312. Wiley.